Elsevier Editorial System(tm) for Medical Engineering & Physics

Manuscript Draft

Manuscript Number: MEP-D-16-00607

Title: Vibration - based Fixation Assessment of Tibial Knee Implants: A Combined In Vitro and In Silico Study

Article Type: Paper

Section/Category: Regular Issue Paper

Keywords: Numerical and Experimental Modal Analysis; Total Knee Replacement; Tibial Implant Loosening Detection; Finite Element Analysis

Corresponding Author: Mr. Steven Leuridan, MSc.

Corresponding Author's Institution: KU Leuven

First Author: Steven Leuridan, MSc.

Order of Authors: Steven Leuridan, MSc.; Quentin Goossens; Tom Vander Sloten; Koen De Landsheer; Hendrik Delport; Leonard Pastrav; Kathleen Denis; Wim Desmet; Jos Vander Sloten

Abstract: The preoperative diagnosis of loosening of cemented tibial knee implants is challenging. This study explored the basic potential of a vibration-based method as an alternative diagnostic technique to assess the fixation state of a cemented tibia implant and establish the method's sensitivity limits and potential for in vitro application. A combined in vitro and in silico approach was pursued. Several loosening cases were simulated. The largest changes in the vibrational behavior were obtained in the frequency range above 1500 Hz. The vibrational behavior was described with two features; the frequency response function and the power spectral density bandpower. Using both features, all experimentally simulated loosening cases could clearly be distinguished from the fully cemented cases. Furthermore, also the location of loosening could be determined. By complementing the experimental work with an in silico study, it was shown that loosening of approximately 14% of the implant surface on the lateral and medial side was detectable with a vibration-based method. Proximal lateral and medial locations on the tibia or locations directly on the implant surface were the most sensitive measurement and excitation locations to assess implant fixation. Vibration-based fixation assessment is a promising alternative technique to assess tibial implant fixation.

KU LEUVEN

Medical Engineering & Physics

To the Editor

OUR REFERENCE
YOUR REFERENCE
LEUVEN 2016-10-24

**COVER LETTER**

Dear Editor

As corresponding author, I wish to submit a paper to Medical Engineering & Physics. The title is "Vibration – based Fixation Assessment of Tibial Knee Implants: A Combined In Vitro and In Silico Study", by Steven Leuridan, Quentin Goossens, Tom Vander Sloten, Hendrik Delport, Leonard Pastrav, Kathleen Denis, Wim Desmet and Jos Vander Sloten. On behalf of the co-authors I confirm that the material within has not been and will not be submitted for publication elsewhere. All authors have made substantial contributions, have read the manuscript and concur with the content.

Sincerely yours

Steven Leuridan

**Ir. Steven Leuridan**, DOCTORAL STUDENT
TEL. + 32 476 75 78 79
steven.leuridan@kuleuven.be

***Declaration form**

| | |
|---|---|
| **Journal**: MEDICAL ENGINEERING & PHYSICS | **Title of Paper**: Vibration – based Fixation Assessment of Tibial Knee Implants: A Combined In Vitro and In Silico Study |

## Declarations

The following additional information is required for submission. Please note that failure to respond to these questions/statements will mean your submission will be returned to you. If you have nothing to declare in any of these categories then this should be stated.

**Conflict of interest**
All authors must disclose any financial and personal relationships with other people or organisations that could inappropriately influence (bias) their work. Examples of potential conflicts of interest include employment, consultancies, stock ownership, honoraria, paid expert testimony, patent applications/registrations, and grants or other funding.

**Ethical Approval**
Work on human beings that is submitted to *Medical Engineering & Physics* should comply with the principles laid down in the Declaration of Helsinki; Recommendations guiding physicians in biomedical research involving human subjects. Adopted by the 18th World Medical Assembly, Helsinki, Finland, June 1964, amended by the 29th World Medical Assembly, Tokyo, Japan, October 1975, the 35th World Medical Assembly, Venice, Italy, October 1983, and the 41st World Medical Assembly, Hong Kong, September 1989. You should include information as to whether the work has been approved by the appropriate ethical committees related to the institution(s) in which it was performed and that subjects gave informed consent to the work.

**Competing Interests**

We have read and understood Medical Engineering & Physics policy on declaration of interests and declare that we have no competing interests

**Please state any sources of funding for your research**

IWT scholarship (Agency for Technology and Innovation, Flanders) (SL), Impulse Fund KU Leuven (QG)

**DOES YOUR STUDY INVOLVE HUMAN SUBJECTS? Please cross out whichever is not applicable.**

~~**Yes**~~

**No**

**If your study involves human subjects you MUST have obtained ethical approval.**
**Please state whether Ethical Approval was given, by whom and the relevant Judgement's reference number**

\

**This information must also be inserted into your manuscript under the acknowledgements section prior to the References.**

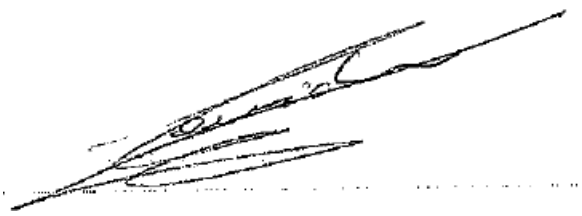

## Referee Suggestions

Title article: Vibration – based Fixation Assessment of Tibial Knee Implants: A Combined In Vitro and In Silico Study

1. **Marie-Christine Ho Ba Tho**
   Roberval Laboratory, Université de Technologie de Compiègne (U.T.C)
   Biomécanique et Bioingénierie
   E-mail: hobatho@utc.fr
   Address: CNRS 7338, BP 20529, 60205 Compiègne, France
2. **Mehrez Loujaine**
   Sonny Astani Department of Civil and Environmental Engineering, University of Southern California (USC)
   E-mail: lmehrez@usc.edu
   Address: Kaprielian Hall, Suite 210; 3620 S. Vermont Avenue; Los Angeles, CA 90089-2531, USA
3. **Edward Valstar**
   Leids Universitair Medisch Centrum, University of Leiden.
   E-mail: e.r.valstar@lumc.nl
   Address: Albinusdreef 2, 2333 ZA Leiden
4. **Cathérine Ruther**
   Departement of Orthopedics, University Medicine Rostock.
   E-mail: catherine.ruther@med.uni-rostock.de
   Address: Deberaner Strasse 142, D-18057 Rostock, Germany
5. **James L. Cunningham**
   Department of Mechanical Engineering, University of Bath
   E-mail: j.l.cunningham@bath.ac.uk
   Address: North Rd, Bath BA2 7AY, United Kingdom.

***Highlights (for review)**

Highlights

- The bone-implant vibrational behavior is sensitive to implant fixation changes
- The frequency range above 1500 Hz is most sensitive to fixation changes
- Measurement locations at the proximal bone or on the implant are most suitable
- Loosening and the location thereof can be determined using vibrational features

# Vibration – based Fixation Assessment of Tibial Knee Implants: A Combined In Vitro and In Silico Study

Steven Leuridan[a]; steven.leuridan@kuleuven.be

Quentin Goossens[a,b]; quentin.goossens@kuleuven.be

Tom Vander Sloten[b]; tom.vander.sloten@gmail.com

Koen De Landsheer[b]; koen_dl3@hotmail.com

Hendrik Delport[a]; hendrik.delport@telenet.be

Leonard Pastrav[b]; leonard.pastrav@kuleuven.be

Kathleen Denis[b]; kathleen.denis@kuleuven.be

Wim Desmet[c]; wim.desmet@kuleuven.be

Jos Vander Sloten[a]; jos.vandersloten@kuleuven.be

a) KU Leuven, Department of Mechanical Engineering, Biomechanics Section. Celestijnlaan 300C - box 2419, 3000 Leuven, Belgium

b) KU Leuven, Department of Mechanical Engineering Technology, Andreas Vesaliusstraat 13 – box 2600, 3000 Leuven, Belgium

c) KU Leuven, Department of Mechanical Engineering, Production Engineering, Machine Design and Automation Section. Celestijnlaan 300C - box 2420, 3000 Leuven, Belgium

**Abstract**

The preoperative diagnosis of loosening of cemented tibial knee implants is challenging. This study explored the basic potential of a vibration–based method as an alternative diagnostic technique to assess the fixation state of a cemented tibia implant and establish the method's sensitivity limits and potential for in vitro application. A combined in vitro and in silico approach was pursued. Several loosening cases were simulated. The largest changes in the vibrational behavior were obtained in the frequency range above 1500 Hz. The vibrational behavior was described with two features; the frequency response function and the power spectral density bandpower. Using both features, all experimentally simulated loosening cases could clearly be distinguished from the fully cemented cases. Furthermore, also the location of loosening could be determined. By complementing the experimental work with an in silico study, it was shown that loosening of approximately 14% of the implant surface on the lateral and medial side was detectable with a vibration-based method. Proximal lateral and medial locations on the tibia or locations directly on the implant surface were the most sensitive measurement and excitation locations to assess implant fixation. Vibration-based fixation assessment is a promising alternative technique to assess tibial implant fixation.

**Keywords:** Numerical and Experimental Modal Analysis; Total Knee Replacement; Tibial Implant Loosening Detection; Finite Element Analysis

## 1. Introduction

Total knee replacement (TKR) is a surgical procedure to replace the weight-bearing surfaces of the knee joint with a prosthesis. It is performed for knee diseases such as osteoarthritis or rheumatoid arthritis. TKR has a high incidence; totaling the number of primary knee replacements in the Scandinavian countries, the UK, Spain, Italy and Germany, over 440 000 primary total knee replacements were performed in 2009 [16]. When a cemented prosthesis is used, the fixation of the components to the host bone is based on the use of bone cement. Although literature shows high survival rates, the number of revisions is high, due to the large number of primary TKR's: approximately 5 to 10% of the prostheses need to be replaced within 10 to 15 years [16]. Loosening of a component is one of the main indications for a revision.

The preoperative diagnosis of loosening is a crucial but difficult one. In up to 75% of painful prostheses the cause remains unknown until the time of surgical intervention with microbiological culturing [32]. However, it is important to be able to differentiate aseptic loosening from e.g. infection because the treatment of these entities is radically different.

Currently, the routine investigation method used in the evaluation of TKR's consists of a combination of different techniques such as radiography and nuclear scanning tests. Radiography is used to evaluate prosthesis alignment, fixation, gross polyethylene wear, and quality of periprosthetic bone [4]. Although it is the classic evaluation method, it is also known as subjective, inconclusive and having a low sensitivity/specificity to assess loosening (e.g. for the tibial component, [50] reported a sensitivity of 43% and a specificity of 86%, [30] reported a sensitivity of 83% and a specificity of 72%). Literature shows diverse results for the use of nuclear scanning tests (e.g. bone scintigraphy, digital subtraction arthrography, 18F-FDG-PET) to detect loosening of the tibial component [e.g. 6, 19, 20, 23, 27, 43, 47, 50]. Very obvious loosened tibial prostheses are likely to be detected by these techniques, because of the

osteoblastic proliferation giving rise to tracer uptake; although it is not straightforward to detect slightly loosened prostheses.

Vibration analysis might be an alternative technique for the detection of knee implant fixation. Vibration analysis, a non-destructive testing technique to inspect structural integrity [14, 49], has been successfully used in biomechanics to determine bone mechanical properties [38, 55] and to monitor fracture healing [28, 37]. It is also a promising method to assess the mechanical properties of the implant-bone systems [34]. Vibrational techniques have shown their merit in the detection of loosening [17, 26] of total hip replacement systems. Several features based on the vibration output have been used in the detection of late and early loosening, such as harmonic distortions [17]. Besides the post-operative applications aiming to detect loosening of hip implants, vibration analysis is also used as a tool to aid the surgeon during surgery in determining the endpoint of insertion of cementless hip implants and to avoid peroperative fractures. It was shown that vibration or impact analysis allows for a reliable detection of the endpoint of insertion, both in vitro [2, 9, 21, 24, 31, 41, 44], ex vivo [35] and in an in vivo setting [25, 40]. The assessment of the stability of cemented knee implants by vibration analysis however, is currently a domain less explored.

This study presents a combined in vitro and in silico feasibility study to determine the potential of using vibrational information to assess the fixation of the tibial component of a TKR. Several clinically relevant loosening cases were first replicated experimentally in vitro. Different excitation and measurement locations and vibrational data features were proposed. Excitation and measurement locations expected to have more limited skin and fat tissue in vivo were selected to optimize accessibility in a post-operative setting. Furthermore, given the recent advances in instrumented implants for orthopedic applications (e.g. hip implant [10, 29, 46] or knee implant [13]), possibilities were likewise explored for the use of a vibration-based method under the assumption that an implant could be instrumented. These results were then complemented with a FE model to further understand the sensitivities of the results to different

parameters that were difficult to vary experimentally and to establish the detection limits of a vibration – based technique.

## 2. Methods

### *2.1 In Vitro Study*

#### *2.1.1 Sample Preparation*

Five left fourth-generation composite tibias (Sawbones Model 3401, Sawbones, Vashon Island, WA, USA) were used in combination with a cemented tibial knee implant (Genesis II, Smith & Nephew, Memphis, TN, USA). The replicate bone models were prepared by the same experienced surgeon following standard procedure while using manufacturer provided instruments. Cementation was performed using Refobacin Bone Cement R (Biomet, Warsaw, IN, USA). Four different fixation cases were replicated experimentally; two samples were prepared to have an optimal, fully cemented fixation between bone and implant, one sample was prepared to simulate peripheral loosening between cement and implant (approx. 50% of the implant surface was loose) and two samples were prepared to simulate loosening on the medial, respectively lateral side between cement and implant (approx. 35% of the implant surface was loose for both cases). Medial and lateral loosening has frequently been reported in clinical practice [53]. Fig. 1 illustrates the three loosened cases. Loosening was realized experimentally by interposing a thin plastic film (thickness of approx. 40 µm), smeared with beeswax on both sides, between cement and implant at the areas where cement–implant interlock was to be prevented. The film was removed after the cement was fully cured. All cases felt mechanically stable after preparation.

#### *2.1.2 Vibration Analysis*

Three sets of vibrational data were collected. Firstly, experimental modal analyses were carried out on four unprepared composite tibia samples and on the two fully cemented implant–tibia samples *(modal analysis set)*. Each sample was mounted horizontally using soft elastic straps in order to simulate free–free boundary conditions [52]. Fig. 2 shows the experimental setup. Three unidirectional lightweight accelerometers (PCB A352A24, PCB Piezotronics, Depew, NY, USA, weight 0.8 g) were attached to the specimen using beeswax in three orthogonal directions. The sample was excited using a modal impaction

hammer instrumented with a force cell (PCB 086C03). Impaction was performed in the direction normal to the specimen surface at 48 locations (roving hammer testing). Excitation locations were evenly distributed across the sample. Five measurements were averaged for each location. These input–output measurements resulted in a measurement set of 144 Frequency Response Functions (FRFs) per test sample. Mode shapes and resonance frequencies were extracted using the Polymax algorithm available in the modal analysis software package (LMS Test Lab, Siemens PLM Software, Leuven, Belgium) in a range of 50 – 4500 Hz, encompassing the first 12 flexible mode shapes. The frequency range was determined during pilot testing and was based on the force autopower spectrum to ensure sufficient mechanical energy was injected into the system in the band of interest. The experimental modal results obtained for the unprepared composite tibia samples were used to update the cortical analogue material properties of the composite tibia FE model to ensure the experimentally measured vibrational behavior correlated well with the numerically predicted vibrational behavior. The experimental modal results obtained for the fully cemented implant – tibia samples were used to again ensure the vibrational behavior of the numerical model including a fully cemented tibial implant accurately reflected the experimental behavior.

Secondly, a set of direct FRFs was collected on the tibia surface for all five implant–tibia constructs (*post-operative diagnostic set*). Direct FRFs are obtained by exciting the structure and measuring the structure's response at the same location in the same direction (here named *x-direction*). Three locations were selected on the surface of the composite tibia; one location on the medial malleolus (MM), one location proximally on the medial side of the tibial plateau (PM) and one location proximally on the lateral side of the tibial plateau (PL). Fig. 3(A) illustrates these locations. These locations were picked as they are expected to have more limited skin and fat tissue coverage compared to other bony tibia locations in vivo, and thus might be easier to access in a post-operative setting. The excitation direction, by impaction using a modal hammer (PCB 086C03), and measurement direction of the acceleration (PCB A352A24) were

normal to the location's surface. Free–free conditions were simulated as these boundary conditions mimic closely the in vivo situation [55]. Only one accelerometer was used, which was relocated for every measurement to the location of interest. Five measurements were averaged for each location. This measurement set was used to assess the potential of a vibration–based technique to discriminate between the different fixation cases in a configuration similar to a possible post-operative test setting.

Thirdly a set of vibrational measurements was collected on the tibial implant surface for all five implant-tibia constructs (*instrumented implant set*). Data were collected at 9 locations on the implant surface (fig. 3(A top)) in the direction normal to the implant surface (*z-direction*). Impact excitation was performed using a modal hammer (PCB 086C03). Direct FRFs at all implant locations were recorded as well as the FRFs obtained from the acceleration response at all 9 implant locations to an excitation at implant location 5 (*5X FRFs*). Again, only one lightweight accelerometer (PCB A352A24) was used, which was relocated to the point of interest for every measurement. Five measurements were averaged for each measurement; free–free boundary conditions were simulated. Although these locations are not directly accessible post-operative, this data set was collected to evaluate the potential of a vibration–based method when integrated in an instrumented implant.

In addition to these three data sets, the linearity of the different implant–tibia fixation constructs was verified by performing a reciprocity check [15] on the implant–tibia construct between locations 2 and 8 on the implant surface. Severe loosening is often characterized by a nonlinear response to a vibrational input signal [17]. Reciprocity was verified by calculating the mean square distance (MSD) between the autopowers of the reciprocal FRFs [15].

Data acquisition and conditioning for all measurements was performed using a spectral analyzer (LMS SCADAS Mobile, Siemens PLM Software, Leuven, Belgium) and acquisition and processing software (LMS Test Lab). The sampling frequency was set to 20.48 kHz.

### *2.1.3 Feature Definitions and Data Processing*

*Modal analysis set.* Mode shapes and resonance frequencies were extracted in the 50 – 4500 Hz frequency band. The experimental mode shapes were compared to the mode shapes obtained from their FE counterparts (respectively FE models of an unprepared tibia and of a fully cemented implant–tibia construct) using the Modal Assurance Criterion (MAC) [1]:

$$MAC = \frac{\left|\{\psi_{qExp}\}^H\{\psi_{qNum}\}\right|^2}{\{\psi_{qExp}\}^H\{\psi_{qExp}\}\{\psi_{qNum}\}^H\{\psi_{qNum}\}}$$

The resonance frequency difference between the experimental and corresponding FE model was expressed as a percentage difference.

*Post-operative diagnostic set.* Two vibrational data features were used to assess the fixation state of the tibial implant; the direct FRFs and the Power Spectral Density (PSD) bandpower, both in the 1500 – 4500 Hz frequency interval. The FRFs obtained from the loosened implant–tibia constructs at the PM, PL and MM locations were compared to the FRFs obtained at the same locations on the fully cemented implant–tibia constructs using the Frequency Assurance Criterion (FRAC) [1]:

$$FRAC = \frac{\left|\sum_{f_1=1500}^{f_2=4500} H_{pq}(f)_{ref}{H_{pq}}^*(f)_{loose}\right|^2}{\sum_{f_1=1500}^{f_2=4500} H_{pq}(f)_{ref}{H_{pq}}^*(f)_{ref}\sum_{f_1=1500}^{f_2=4500} H_{pq}(f)_{loose}{H_{pq}}^*(f)_{loose}}$$

The PSD band powers were used to calculate a ratio between the PM and the PL (or vice versa) band power obtained on the same construct (*PL–PM PSD ratio or PM–PL PSD ratio*). Ratios markedly different from 1 would be indicative of a local loss in stiffness on one side resulting in larger accelerations for the same unit input on that side and thus higher amplitude levels in the PSD.

$$PL - PM\ PSD\ ratio = \frac{\sum_{f_1=1500}^{f_2=4500} PSD_{pq}(f)_{PL}}{\sum_{f_1=1500}^{f_2=4500} PSD_{pq}(f)_{PM}}$$

*Instrumented implant set*. The FRFs and PSD bandpowers were used as data features, again both in the 1500 – 4500 Hz frequency interval, obtained from the direct measurements as well as from the 5X measurements. The FRFs of the loosened constructs were compared to the corresponding FRFs of the fully cemented constructs using the FRAC. Similarly, ratios were calculated between the bandpowers obtained from the loosened constructs and the fully cemented constructs for corresponding input – output measurements (*PSD ratio*).

$$PSD\ ratio = \frac{\sum_{f_1=1500}^{f_2=4500} PSD_{pq}(f)_{loose}}{\sum_{f_1=1500}^{f_2=4500} PSD_{pq}(f)_{ref}}$$

All data processing was performed in Matlab (Matlab, Natick, MA, USA).

## *2.2 In Silico Study*

### *2.2.1 FE Model Construction & Composite Tibia Material Parameter Updating*

A composite tibia sample was CT scanned (Aquillon One, Toshiba Medical Systems Corporation, Otawara, Japan) with a 0.5 mm slice thickness. A FE model was built based on the CT scan data using Mimics (Materialise NV, Leuven, Belgium) and MSC Patran (MSC Software, Newport Beach, CA, USA). Cortical and cancellous bone analogue regions were assigned to the FE models based on grey values. The tibia model consisted of 31,078 quadratic tetrahedral elements with an average element size of 3.5 mm. The element size was determined based on a convergence analysis performed on the model. A transversely isotropic material model was selected for the cortical bone analogue region; an isotropic material model was used for the cancellous bone region. The third material axis of the transversely isotropic material model was parallel to the anatomical axis of the composite tibia. The elastic material constants of the cortical analogue were determined by updating the unprepared tibia FE model's material parameters. The material parameters were updated by minimizing the average and maximal difference between the experimentally measured and numerically predicted resonance frequencies of the first 12 correlated flexible mode shapes [22]. The starting values of the cortical analogue material parameters were; $E_{11}$ (= $E_{22}$) = 10.00 GPa (Transverse Young's moduli), $E_{33}$ = 16.00 GPa (Longitudinal Young's Modulus), $G_{23}$ (=$G_{31}$) = 3.30 GPa, $\nu_{12}$ = 0.26, $\nu_{23}$ = 0.26, and $\rho$ = 1.64 g/cc [18, 48]. The elastic material properties of the elements in the trabecular region were not updated. Following values were used; E = 155 MPa, $\nu$ = 0.3 and $\rho$ = 2.70E-1 g/cc [48]. The cortical and trabecular material densities were updated by matching the measured mass of the composite tibia to the calculated mass of the FE model.

The implant was 3D scanned (MC16, Coord3, Turin, Italy) after which the resulting point cloud was further processed in 3-Matic (Materialise NV, Leuven, Belgium) and MSC Patran to construct the FE model. The implant model consisted of 6,665 quadratic tetrahedral elements, isotropic material properties were assigned to the elements (E = 113.8 GPa, $\nu$ = 0.342, $\rho$ = 4.43 g/cc [3]). The tibia was prepared virtually in such a way so to reflect the experimental surgical preparation as closely as possible. Firstly,

the tibial plateau was virtually resected after which the implant model was subtracted from the tibia. Tibia and implant model were then combined and a cement layer of approx. 3.5 mm was defined between the tibia and implant surfaces. Isotropic material parameters ($E = 2.28GPa$, $\nu = 0.3$, $\rho = 1.18$ g/cc) were used for the cement layer [51]. A glued contact definition was used between cement-implant and cement-tibia throughout all simulations. The final implant–tibia model consisted of 50,913 elements and is shown in Fig. 3(B).

*2.2.2 Fixation Cases Definition*

In order to determine the detection limits of a vibration based fixation assessment method and establish a minimally detectable loosened area, 21 cases with a varying degree of fixation were simulated using the implant-tibia FE model; one optimally cemented, fully fixed case and 20 cases with different partially loosened regions. Fig. 4 gives an overview of the loosened cases and shows the cumulative area that was detached for every case. Loosening between cement and implant as well as between cement and bone has been reported clinically [54]. To assess whether the proposed vibration method was more prone to detect loosening at the cement–bone interface or loosening at the cement–implant interface, both scenarios were simulated for all partially loosened cases. Damping is an important concern when vibrational techniques are applied in trying to solve biomechanical problems such as loosening detection [47]. To determine whether the vibrational method still holds promise in a more damped environment, two damping levels were used for the simulations; a modal damping factor of 1.5% for all modes (similar to the average damping of 1.37% which was measured experimentally on the composite tibias during pilot testing) and a damping factor of 5%, which is comparable to the damping encountered in cadaveric or fresh frozen bone [8]. Fig. 5 provides an overview of all combinations simulated.

*2.2.3 Feature Definition and Data Processing*

The first 20 resonance frequencies and their corresponding mode shapes were calculated by numerical modal analysis for all cases (MSC Nastran, MSC Software, Newport Beach, CA, USA). Furthermore, in

order to replicate the features that were used in the second and third experimental data set, FRFs were synthesized at comparable locations and in the same directions as their experimental counterparts. The locations on the tibia, replicating the situation where the technique would be used as a postoperative diagnostic tool, were exactly the same. The locations on the implant, replicating the situation in which an implant would be instrumented (*instrumented implant set*), were somewhat altered with respect to the experimental locations as a preliminary numerical sensitivity study indicated that implant locations which were more sensitive to detect interface loosening were available. Fig 3(B top) depicts these locations on the implant. The mode shapes and resonance frequencies were used in the cortical analogue material updating process. The PSD band power feature was calculated based on the synthesized FRFs. Analog to the experimental case, the 1500 – 4500 Hz frequency band was used for the comparing the FRFs & PSD band powers. FRFs were compared between the fully cemented case and the different loosened cases using the FRAC. Ratios were calculated between the corresponding PSD band powers of the different partially loosened cases and the fully cemented case. In addition to the FRFs and PSD powers, also the differences in resonance frequency shifts were studied for the numerical models to gain further insight in the fundamental vibrational characteristics of the different cases.

### *2.2.4 Operational and Environmental Variability*

Besides changes in fixation, other sources of variability may also have an influence on the vibrational behavior of an implant-tibia construct. The resection cut angle and cement layer thickness are operational parameters that may show slight variation due to the surgeon's manipulation [11]. The influence on the resonance frequencies with 4 different cutting angles (1.6° degrees difference medial, lateral, anterior and posterior from the neutral cutting angle) was numerically investigated in combination with a fully cemented implant-tibia case with a cement layer thickness of approx. 3.5 mm [36]. The effect of two cement layer thicknesses (3.5 and 7 mm) on the resonance frequencies of a fully cemented implant-tibia case with a neutral angle resection was likewise determined.

Furthermore, as the vibrational method is envisioned to be used as a diagnostic follow up tool, other parameters besides the bone–cement or cement–implant interface may change over time. Important variability may be introduced by changes in bone material properties over time, e.g. due to aging [39] or progressing osteoporosis. A sensitivity analysis was therefore performed to assess the impact changing material properties have on the resonance frequencies of an implant-tibia construct. This sensitivity analysis was performed on a fully cemented implant-tibia FE model with a cement layer of 3.5 mm resected under a neutral angle. The changes in resonance frequencies are reported as the ratio of a percentage difference in resonance frequencies over a percentage difference of the parameter of interest.

## 3. Results

### *3.1 Experimental In Vitro Study*

#### *3.1.1 Post-Operative Diagnostic Set*

Fig 6 shows the direct FRFs measured at the medial malleolus for a fully cemented case and the three loosened cases. Very little change was observed in the frequency band below 1500 Hz. Table 1 lists the FRAC values obtained by comparing the direct FRFs of the different loosened cases with the fully cemented case at all three tibia measurement locations. The average FRAC values between the two fully cemented cases at identical measurement locations were 0.95 (SD 0.01). Flagging the FRAC values outside a three standard deviation confidence interval (FRAC < 0.92) or even outside a more restrictive ten standard deviation confidence interval (FRAC < 0.85) as a loosened case, all three cases were correctly classified as loosened based on their vibrational FRF signature at all three measurement locations. Furthermore, the PL – PM (or PM – PL) PSD ratio increased notably at the loosened side for the unilateral loosened cases (table 1), allowing localization of the loosened region for these cases.

#### *3.1.2 Instrumented Implant Set*

Table 2 lists the FRAC values obtained by comparing corresponding FRFs measured on the fully cemented case and on the different loosened cases. The tabulated FRAC values relate to the FRFs with direct excitation at location number 5 and acceleration measurement at the different implant locations (5X FRFs). Again all loosened cases were correctly classified as loosened when a similar threshold was used (FRAC < 0.92 or <0.85). Loosening was detectable at all implant measurement locations. The FRAC values between corresponding fully cemented and loosened direct FRFs at all measurement locations were similar to the 5X results, with an average difference in the FRAC value of 0.01 (SD 0.15). Fig. 7 shows the different PSD ratios (between fully cemented–loosened cases) for the three loosened cases at all 9 measurement locations. The average PSD ratio between the two fully cemented cases was 0.95 (SD 0.10). Locations with a PSD ratio above the 1.25 mark (i.e. outside a three standard deviation confidence

interval) corresponded to those measurement locations closest to the areas where the implant was detached in the different loosened cases.

*3.1.3 Linearity Check*

The largest MSD (in % of total energy) was 0.5%, which confirms all experimental composite – tibia implant constructs exhibited strictly linear behavior for the cases tested in this study.

*3.2 In Silico Study*

Good correspondence was obtained between the experimental vibrational behavior of the unprepared tibias and their numerical counterpart after updating. The average frequency difference was 5.75% (SD 0.61%) before updating the cortical bone analogue material parameters and was reduced to 1.42% (SD 0.92%) after updating. The material properties after updating were; $E_{11}$ (= $E_{22}$) = 9.88 GPa, $E_{33}$ = 14.01 GPa, $G_{23}$ (=$G_{31}$) = 3.83 GPa, $\nu_{12}$ = 0.26, $\nu_{23}$ = 0.26, and $\rho$ = 1.64 g/cc. The average MAC value was 0.81 (SD 0.04) after updating. The density of the trabecular bone analog was unchanged at $\rho$ = 2.70E-1 g/cc. These material parameter values were subsequently used for the FE model which included the tibial implant. An average resonance frequency difference of 1.70% (SD 1.40%) and average MAC value of 0.79 (SD 0.05) were found between the experimental implant–tibia construct and the FE model, thus ensuring the FE model mimicked the experimental behavior closely.

The results from the FE model corroborated well with the experimental findings. Fig. 8 shows the resonance frequency difference for the different cases with partial loosening between cement and implant. Only the largest of loosened cases resulted in major differences in the frequency range below 1500 Hz. The resonance frequency differences when loosening occurred between cement and bone were on average 1.2 percentage points greater (max. 9.8%).

*3.2.1 Post – Operative Diagnostic Set: Sensitivity Limits*

Fig. 9(A) schematically presents the results for all three tibia measurement locations when the FRAC values were calculated between corresponding synthesized FRFs of the fully cemented FE model and the cases with partial loosening between cement and implant. All cumulative loosened areas which resulted in a FRAC value below 0.85 were marked, both in case of a simulated 1.5% and 5% modal damping. Cases with loosened areas of 14% of the surface were detected (L2, M2 on fig.4(A)). Fig 9(B) shows the companion results obtained when loosening was simulated between the cement–bone interface.

*3.2.2 Instrumented Implant Set: Sensitivity Limits*

Fig. 10 illustrates the results obtained when the synthesized 5X FRFs were used to assess implant loosening. The implant location where the FRAC first dropped below 0.85 as well as the value and location where the maximal PSD ratio was observed for that partial loosening case were annotated. Again, loosening of approx.14% of the surface area was detected (L2, M2), as well as a loosened area of 5.6% on the anterior side (A1 on fig 4(B)) Posterior loosening was more difficult to determine. Fig. 11 illustrates the PSD ratios and marks all PSD ratios > 1.95. Similar to the experimental results, locations with higher PSD ratios correlated well with nearby loosened areas.

*3.2.3 Operational and Environmental Variability*

The influence of the different resection angles on the vibrational behavior was limited to an average frequency difference of 0.69% (SD 0.37%) over the frequency range of interest. A similar small effect was noted when the cement layer thickness was doubled, with an average frequency difference of 0.54% (SD 0.41%).

Alterations to the bone material parameters had an important effect on the resonance frequencies, as demonstrated in table 3. The cortical bone density, E33 modulus and G13 shear modulus were the most influential parameters. Interestingly enough, changes in the bone material parameters have an important effect also in the lower frequency range, possibly allowing discriminating these changes from observed changes in the vibrational behavior attributable to loosening.

## 4. Discussion & Conclusions

The main goal of this study was to explore the basic potential of a vibration–based method to assess the fixation state of a cemented tibia implant and establish the method's sensitivity limits. Qi et al. determined these limits for hip implants [42]. A combined in vitro and in silico approach was pursued. The in vitro work allowed to experimentally verify the numerical work, ensured the practical feasibility of the method and allowed assessing which types of features could be used (linear or nonlinear), as the latter are typically more difficult to simulate in silico. Although nonlinear features have shown to be sensitive to loosening in hip implant applications [17], the implant–tibia constructs used in this study did not show any nonlinear behavior. Possibly the experimental loosening cases were not yet severe enough for this behavior to manifest itself. The complementary numerical work allowed establishing sensitivity limits and assessing the influence of damping on the results.

Damping was shown to have a non-trivial influence on the detectability of loosening with the proposed method, especially for the *Post-Operative Diagnostic Set* (fig. 9). Whereas in a lightly damped environment, even small loosening could be detected at all three measurement locations (PM, PL and MM), this ceased to be true in the more heavily damped case. Only the largest loosening cases were detectable at MM. The PM and PL measurement locations were more promising, especially when both were combined. Together, they showed good sensitivity to lateral and medial loosening (PL was more sensitive to lateral loosening and vice versa), as well as anterior loosening. Posterior loosening was more difficult to detect, likely due to the decreased implant area that is loosened for these cases. Bone–cement loosening was generally easier to detect than cement–implant detachment. Future development work should focus on PM–PL combination measurements. An important challenge will be coping with the requirement that the sensory equipment needs to be able to excite and measure the implant – bone system through the skin in a frequency range above 1500 Hz. Promising alternatives to accelerometers have been proposed which may help achieving this objective (e.g. ultrasound [2, 45]).

The in vitro and numerical work for the *Instrumented Implant Set* showed promising results for the ability to detect small loosened cases (fig. 10). Damping was less influential on the detection sensitivity in an instrumented implant setup, although higher FRAC values were typically attained in the more heavily damped cases. Furthermore, increases in PSD bandpower, as expressed by the PSD ratio, at certain implant measurement locations allowed localization of the loosened regions. Although the effect of important sources of variability such as material parameters on the vibrational behavior of the tibia was investigated, the influence of other parameters such as; cortical bone thickness, density distributions, shape changes… could likewise be assessed in future work using techniques like statistical shape modelling [5] or Monte Carlo simulations [33].

Implant location 5 was chosen as excitation location as this location was situated above the implant peg, which could be spacious enough to hold a miniaturized excitation system, similar to the concept presented by Ruther et al [46]. Measurement sensor integration in the implant could possibly be realized using piezo patches [7]. If only a selection of candidate implant locations could be instrumented, locations 2 and 8 would be most interesting if medial or lateral loosening is of main concern, whereas locations 3 and 4 would be prime candidates to detect anterior or posterior loosening.

Describing the vibrational behavior of a structure by the resonance frequencies and mode shapes offers the most complete characterization of the structure under test. However, determining the mode shapes requires a rich data set of multiple FRFs as well as manual input from the user during the parameter estimation process. Other easier to acquire features were proposed to assess the different fixation states as neither acquiring a full data set of FRFs is feasible in a post - operative setting, nor is the expected uncertainty due to the user input beneficial when an automated implementation of the proposed technique is envisioned. The FRF and PSD bandpower features proposed in this study proved to be adequate in describing the changes in vibrational behavior between the different fixation cases. More robust estimation of these spectra may be advantageously for this technique [12] when implemented in vivo. The increase in PSD bandpower for loosened cases can be explained by the occurrence of mode shapes which

show local, high amplitude deformational behavior (Fig. 12). As this deformation is largest in the longitudinal direction, this also elucidates the high sensitivity to loosening in an instrumented implant setting. An important limitation is that a reference measurement, preferably taken shortly after surgery, must be available for comparison.

A vibration based technique using simple features holds promise in assessing the fixation state of tibial cemented implants, either as a post-operative tool or in an instrumented implant implementation.

**Acknowledgements**

Steven Leuridan was funded by a scholarship of IWT (Agency for Technology and Innovation, Flanders). Quentin Goossens was supported by the KU Leuven Impulse Fund.

**Conflict of interest:**

We have read and understood Medical Engineering & Physics policy on declaration of interest and declare that we have no completing interest

**Ethical approval:** None

411 **References**

412 [1] Allemang RJ. The Modal Assurance Criterion – Twenty Years of Use and Abuse. 2003 Sound and
413 Vibration 37(8), 14-23 doi:10.1016/j.proeng.2012.09.551

414 [2] Alshuhri AA, Holsgrove TP, Miles AW, Cunningham JL. Development of a non-invasive diagnostic
415 technique for acetabular component loosening in total hip replacements. Med Eng Phys. 2015
416 Aug;37(8):739-45. doi: 10.1016/j.medengphy.2015.05.012.

417 [3] ASM Matweb, 29 June 2016 http://asm.matweb.com/search/SpecificMaterial.asp?bassnum=MTP643

418 [4] Baré J., MacDonald S.J., Bourne R.B., 2006. Preoperative evaluations in revision total knee
419 arthroplasty. Clinical Orthopaedics and Related Research. 446, 40-44. doi:
420 10.1097/01.blo.0000218727.14097.d5

421 [5] Campoli G, Baka N, Kaptein BL, Valstar ER, Zachow S, et al. (2014). Relationship between the shape
422 and density distribution of the femur and its natural frequencies of vibration. J Biomech 47: 3334-3343.
423 http://dx.doi.org/10.1016/j.jbiomech.2014.08.008

424 [6] Chew C.G., Lewis P., Middleton F., Van den Wijngaard R., Deshaies A., 2010. Radionuclide
425 arthrogram with SPECT/CT for the evaluation of mechanical loosening of hip and knee prostheses. Ann
426 Nucl Med. 24, 735-743. doi: 10.1007/s12149-010-0419-1

427 [7] Correia V; Sencadas V; Martins MS; Ribeiro C; Alpuim P; Rocha JG; Morales I; Atienza C; Lanceros
428 Mendez S, 2013. Piezoresistive sensors for force mapping of hip-prostheses. Sensors and Actuators A:
429 Physical, 2013 Jun; 195(1): 133-138. doi:10.1016/j.sna.2013.03.013

430 [8] Couteau B, Hobatho MC, Darmana R, Brignola JC, Arlaud JY (1998) Finite element modelling of the
431 vibrational behaviour of the human femur using CT-based individualized geometrical and material
432 properties. J Biomech 31: 383-386. http://dx.doi.org/10.1016/S0021-9290(98)00018-9

[9] Cristofolini, L., Varini E., Pelgreffi I., Cappello A., Toni A., 2006. Device to measure intra-operatively the primary stability of cementless hip stems. Medical Engineering & Physics. 28(5): pp. 475-82. http://dx.doi.org/10.1016/j.medengphy.2005.07.015

[10] Damm P, Graichen F, Rohlmann A, Bender A, Bergmann G. Total hip joint prosthesis for in vivo measurement of forces and moments. Med Eng Phys. 2010 Jan;32(1):95-100. doi: 10.1016/j.medengphy.2009.10.003. http://dx.doi.org/10.1016/j.medengphy.2009.10.003

[11] Denis K, Van Ham G, Bellemans J, Labey L, Sloten JV, Van Audekercke R, Van der Perre G, De Schutter J. How correctly does an intramedullary rod represent the longitudinal tibial axes? Clin Orthop Relat Res. 2002 Apr;(397):424-33. doi: 10.1097/00003086-200204000-00050

[12] Díaz-Pérez F, García-Nieto E, Ros A, Claramunt R. Best estimation of spectrum profiles for diagnosing femoral prostheses loosening. Med Eng Phys. 2014 Feb;36(2):233-8. doi: 10.1016/j.medengphy.2013.11.005.

[13] D'Lima DD, Patil S, Steklov N, Colwell CW Jr. The 2011 ABJS Nicolas Andry Award: 'Lab'-in-a-knee: in vivo knee forces, kinematics, and contact analysis. Clin Orthop Relat Res. 2011 Oct;469(10):2953-70. doi: 10.1007/s11999-011-1916-9.

[14] Farrar C, Worden K, An introduction to structural health monitoring, Phil. Trans. R. Soc. A 15 February 2007 vol. 365 no. 1851 303-315. doi: 10.1098/rsta.2006.1928

[15] Farrar, CR., Worden, K. Structural health monitoring: a machine learning perspective. ISBN: 978-1-119-99433-6 pp.251-252 doi: 10.1002/9781118443118

[16] Frost & Sullivan European Orthopaedic Devices Market Outlook , april 2011

[17] Georgiou A.P., Cunningham J.L., 2001. Accurate diagnosis of hip prosthesis loosening using a vibrational technique. Clin. Biomech. 16, 315-323. http://dx.doi.org/10.1016/s0268-0033(01)00002-x

[18] Grassi L, Vaananen SP, Amin Yavari S, Weinans H, Jurvelin JS, et al. (2013) Experimental validation of finite element model for proximal composite femur using optical measurements. J Mech Behav Biomed Mater 21: 86-94. doi: 10.1016/j.jmbbm.2013.02.006

[19] Gratz S., Höffken H., Kaiser J.W., Behr T.M., Strosche H., Reize P., 2009. Nuklearmedizinische Diagnostik bei schmerz-hafter Knieprothese. Radiologe. 49, 59-67. doi:10.1007/s00117-008-1703-0

[20] Gravius S., Gebhard M., Ackermann D. et al., 2010. Analysis of (18)F-FDG uptake pattern in PET for diagnosis of aseptic loosening versus prosthesis infection after total knee arthroplasty A prospective pilot study. Nunklearmedizin-Nuclear Medicine. 49 (3), 115-123. doi: 10.3413/nukmed-0278

[21] Henys P., Capek L., Fencl J., Prochazka E. Evaluation of acetabular cup initial fixation by using resonance frequency principle. Proceedings of the Institution of Mechanical Engineers, Part H: Journal of Engineering in Medicine, January 2015; vol. 229, 1: pp. 3-8. http://dx.doi.org/10.1177/0954411914561485

[22] Heylen, W., Lammens, S., Sas, P., Modal analysis theory and testing. ISBN 90-73802-61-X pp.6.23 – 6.27

[23] Hirschmann M.T., Konala P., Iranpour F., Kerner A., Rasch H., Friederich N.F., 2011. Clinical value of SPECT/CT for evaluation of patients with painful knees after total knee arthroplasty-a new dimension of diagnostics? BMC Musculoskeletal Disorders. 12 (36), 10p. doi: 10.1186/1471-2474-12-36

[24] Jaecques S., Pastrav C., Zahariuc A., Van der Perre G., 2004. Analysis of the fixation quality of cementless hip prostheses using a vibrational technique. In: Sas P., De Munck M. (Eds.), ISMA 2004, International Conference on Noise and vibration engineering. K.U.Leuven, Leuven, Belgium, pp. 443-456. doi: 10.1115/ESDA2004-58581

476 [25] Lannocca M, Varini E, Cappello A, Cristofolini L, Bialoblocka E. Intra-operative evaluation of
477 cementless hip implant stability: a prototype device based on vibration analysis. Med Eng Phys. 2007
478 Oct;29(8):886-94. Epub 2006 Nov 13. doi: 10.1016/j.medengphy.2006.09.011

479 [26] Li PL, Jones NB, Gregg PJ. Vibration analysis in the detection of total hip prosthetic loosening. Med
480 Eng Phys. 1996 Oct;18(7):596-600. doi:10.1016/1350-4533(96)00004-5

481 [27] Lorberboym M., Feldbrin Z., Hendel D., Blankenberg F.G., Schachter P., 2009. The use of 99mTc-
482 recombinant human annexin V imaging for differential diagnosis of aseptic loosening and low-grade
483 infection in hip and knee prostheses. J Nucl Med. 50(4), 534-7. doi: 10.2967/jnumed.108.059345

484 [28] Lowet G., Van der Perre G., 1996. Ultrasound velocity measurement in long bones: measurement
485 method and simulation of ultrasound wave propagation. J. Biomech. 29, 1255-1262. doi:10.1016/0021-
486 9290(96)00054-1

487 [29] Marschner U, Grätzb H, Jettkantc B, Ruwischd D, Woldte G, Fischera WJ, Clasbrummelf B,.
488 Integration of a wireless lock-in measurement of hip prosthesis vibrations for loosening detection. Sensors
489 and Actuators A: Physical: Volume 156, Issue 1, November 2009, Pages 145–154.
490 http://dx.doi.org/10.1016/j.sna.2009.08.025

491 [30] Marx A., Saxler G., Landgraeber S., 2005. Comparison of subtraction arthrography, radionuclide
492 arthrography and conventional plain radiography to assess loosening of total knee arthroplasty.
493 Biomedizinische Technik, 50, (5) 143 147. doi: 10.1515/BMT.2005.021

494 [31] Mathieu V, Michel A, Flouzat Lachaniette CH, Poignard A, Hernigou P, Allain J, Haïat G. Variation
495 of the impact duration during the in vitro insertion of acetabular cup implants. Med Eng Phys. 2013
496 Nov;35(11):1558-63. doi: 10.1016/j.medengphy.2013.04.005. Epub 2013 Jun 6.

[32] Mayer-Wagner S., Mayer W., Maegerlein S., Linke R., Jansson V., Müller P., 2010. Use of 18F-FDG-PET in the diagnosis of endoprosthetic loosening of knee and hip implants. Arch Orthop Trauma Surg. 130, 1231–1238. doi: 10.1007/s00402-009-1000-z

[33] Mehrez, L., Browne, M., 2012. A numerically validated probabilistic model of a simplified total hip replacement construct. Comput Methods Biomech Biomed Engin 15(8):845-58. doi: 10.1080/10255842.2011.564163

[34] Meredith N., Book K., Friberg B., Jemt T., Sennerby L., 1997. Resonance frequency measurements of implant stability in vivo. A cross-sectional and longitudinal study of resonance frequency measurements on implants in the edentulous and partially dentate maxilla. Clin. Oral Implants Res. 8, 226-233. doi: 10.1034/j.1600-0501.1997.080309.x

[35] Michel A, Bosc R, Sailhan F, Vayron R, Haiat G, 2013. Ex vivo estimation of cementless acetabular cup stability using an impact hammer. Med Eng Phys. 2016 Feb;38(2):80-6. doi: 10.1016/j.medengphy.2015.10.006

[36] Miller MA, Goodheart JR, Izant TH, Rimnac CM, Cleary RJ, Mann KA. Loss of cement-bone interlock in retrieved tibial components from total knee arthroplasties. Clin Orthop Relat Res. 2014 Jan;472(1):304-13. doi: 10.1007/s11999-013-3248-4

[37] Nakatsuchi Y., Tsuchikane A., Nomura A., 1996. Assessment of fracture healing in the tibia using the impulse response method. J. Orthop. Trauma 10, 50-62.

[38] Nokes L.D.M., 1999. The use of low-frequency vibration measurement in orthopaedics. Proc. Instn. Mech. Engrs. 213H: 271-290.

[39] O'Flaherty EJ. Modeling normal aging bone loss, with consideration of bone loss in osteoporosis. Toxicol Sci. 2000 May;55(1):171-88. doi: 10.1093/toxsci/55.1.171

519 [40] Pastrav L.C., Jaecques S.V.N., Jonkers I., Van der Perre G., Mulier M., 2009. In vivo evaluation of a
520 vibration analysis technique for the per-operative monitoring of the fixation of hip prostheses, Journal of
521 Orthopaedic Surgery and Research, 4:10. doi: 10.1186/1749-799X-4-10

522 [41] Pastrav L.C., Jaecques S.V.N., Mulier M., Van der Perre G., 2008. Detection of the insertion end
523 point of cementless hip prostheses using the comparison between successive frequency response
524 functions. Journal of Applied Biomaterials & Biomechanics, 6(1), 23-29.

525 [42] Qi G, Mouchon WP, Tan TE. How much can a vibrational diagnostic tool reveal in total hip
526 arthroplasty loosening? Clin Biomech (Bristol, Avon). 2003 Jun;18(5):444-58. doi:
527 http://dx.doi.org/10.1016/S0268-0033(03)00051-2

528 [43] Reinartz P., 2009. FDG-PET in patients with painful hip and knee arthroplasty: technical
529 breakthrough or just more of the same. Quarterly Journal of Nuclear Medicine and Molecular Imaging. 53
530 (1), 41-50.

531 [44] Rieger JS, Jaeger S, Schuld C, Kretzer JP, Bitsch RG. A vibrational technique for diagnosing
532 loosened total hip endoprostheses: an experimental sawbone study. Med Eng Phys. 2013 Mar;35(3):329-
533 37. doi: 10.1016/j.medengphy.2012.05.007

534 [45] Rowlands A., Duck F.A., Cunningham J.L., 2008. Bone vibration measurement using ultrasound:
535 Application to detection of hip prosthesis loosening, Medical Engineering & Physics, 30(3), 278-284.
536 http://dx.doi.org/10.1016/j.medengphy.2007.04.017

537 [46] Ruther C, Nierath H, Ewald H, Cunningham JL, Mittelmeier W, Bader R, Kluess D. Investigation of
538 an acoustic-mechanical method to detect implant loosening. Med Eng Phys. 2013 Nov;35(11):1669-75.
539 doi: 10.1016/j.medengphy.2013.06.004.

[47] Savarino L., Tigani D., Baldini N., Bochicchio V., Giunti A., Pre-operative diagnosis of infection in total knee arthroplasty: an algorithm. Knee Surg Sports Traumatol Arthrosc. 17(6), 667-75. doi: 10.1007/s00167-009-0759-3

[48] Sawbones, 29 June 2016 http://www.sawbones.com/UserFiles/Docs/biomechanical_catalog.pdf

[49] Sohn, H., C. R. Farrar, Hemez F.M. , Shunk D.D., Stinemates D.W., Nadler B.R., Czarnecki J.J., 2004. A Review of Structural Health Monitoring Literature from 1996-2001,. LA-13976-MS. Los Alamos National Laboratory.

[50] Sterner T., Pink R., Freudenberg L., Jentzen T., Quitmann H., Bockisch A., Löer F., 2007. The role of [18F]fluoride positron emission tomography in the early detection of aseptic loosening of total knee arthroplasty. Int J Surg. 5 (2), 99-104. doi: 10.1016/j.ijsu.2006.05.002

[51] Stolk J, Verdonschot N, Murphy B, Prendergast P, Huiskes R. Finite element simulation of anisotropic damage accumulation and creep in acrylic bone cement. Engineering Fracture Mechanics Volume 71, Issues 4–6, March–April 2004, Pages 513–528 http://dx.doi.org/10.1016/S0013-7944(03)00048-1

[52] Taylor WR, Roland E, Ploeg H, Hertig D, Klabunde R, et al. (2002) Determination of orthotropic bone elastic constants using FEA and modal analysis. J Biomech 35: 767-773. http://dx.doi.org/10.1016/S0021-9290(02)00022-2

[53] Uematsu O, Hsu HP, Kelley KM, Ewald FC, Walker PS. Radiographic study of Kinematic total knee arthroplasty. J Arthroplasty. 1987;2(4):317-26. doi:10.1016/S0883-5403(87)80066-9

[54] Uhlenbrock GD, Püschel V, Püschel K, Morlock MM, Bishop NE. Influence of time in-situ and implant type on fixation strength of cemented tibial trays - a post mortem retrieval analysis. Clin Biomech (Bristol, Avon). 2012 Nov;27(9):929-35. doi: 10.1016/j.clinbiomech.2012.06.008.

562 [55] Van der Perre G., Lowet G., 1996. In vivo assessment of bone mechanical properties by vibration and
563 ultrasonic wave propagation analysis. Bone 18, 29S-35S. doi:10.1016/8756-3282(95)00377-0

**Fig.1**

Illustration of the cement–implant area that was loosened during experimental testing for (A) the peripheral loosening case, (B) the medial loosening case and (C) the lateral loosening case. The loosened areas are marked in grey, the fixed regions are in white.

**Fig. 2**

The test setup for the experimental modal analysis is depicted. Three accelerometers were mounted on the test sample in three orthogonal directions during modal testing. The hammer was roved around to excite the structure at 48 impact locations. The test sample was mounted in free–free conditions.

**Fig. 3**

Side–by–side comparison of the experimental composite tibia (A) and its numerical FE counterpart (B). PM, PL and MM indicate the measurement and excitation locations used to collect the FRFs (in the x-direction) for the *Post-Operative Diagnostic Set.* The measurement and excitation locations used for the *Instrumented Implant Set* are shown on the top images (numbers 1-9) and were measured in the z-direction.

**Fig.4**

The implant area was divided in 10 areas of equal width. Loosening was simulated by progressively detaching larger interface areas from the lateral side towards the center and from the medial side towards the center (A), and from the anterior side towards the center and from the posterior side towards the center (B). As an example; L3 implies that the first three areas taken from the lateral side ware left loose, thus resulting in a cumulative loosened area of approx. 30% of total implant area. All other areas remain fixed. This is similar for the other loosening cases.

**Fig. 5**

Overview of the different cases that were simulated numerically. A total of 82 simulations were carried out.

**Fig. 6**

Amplitude plot of the direct FRFs measured at the medial malleolus (fully cemented, peripheral, medial and lateral loosening cases). Limited sensitivity is noted in the low frequency region (below 1500 Hz), with most changes in vibrational behavior occurring above 1500 Hz.

**Fig. 7**

PSD ratio comparing the PSD bandpower of the peripheral, lateral and medial loosened case to the average PSD bandpower of the fully cemented cases at corresponding implant measurement locations (1-9). An increase in the PSD bandpower is observed for those measurement locations closest to the loosened areas of the different loosened cases, allowing to localize the areas where loosening has occurred. The 3 standard deviation band around the average PSD ratio of the two cemented cases is marked by the dotted line.

**Fig.8**

The resonance frequency differences obtained by comparing results from the FE model of a fully cemented implant-tibia construct to the results from the FE model of the respective loosened case are depicted. The influence of progressive loosening between cement and implant on the resonance frequencies occurring anteriorly (A), posteriorly (B), laterally (C) and medially (D) is shown.

**Fig.9**

The loosened areas that could be detected by comparing the synthesized FRFs of a fully cemented case to the corresponding FRFs synthesized for the different loosening cases, both when a modal damping of 1.5% an 5% is assumed. In general, bone–cement loosening was easier to detect based on the FRFs as smaller loosened areas could be detected and lower FRAC values were generally found for the same loosened area. The FRAC value for the first loosened area for which the FRAC value is below 0.85 is annotated. FRAC values obtained when 1.5% damping is assumed are presented in a full line box, the FRAC values for the 5% damping cases are presented in a dotted line box. E.g. the minimal loosened area between cement and implant at the lateral side that could be detected based on the FRFs measured at the medial malleolus was L2 (with a FRAC value of 0.72) when 1.5% damping was assumed or L5 (with a FRAC value of 0.84) when 5% damping was assumed. Damping typically decreased the sensitivity of FRF-based loosening detection.This effect was most pronounced for the MM measurement location, but damping had less of an influence for the PM and PL measurement locations.

**Fig.10**

The loosened areas that could be detected by comparing synthesized 5X FRFs of a fully cemented case to the corresponding FRFs synthesized for the different loosening cases, both when a modal damping of 1.5% an 5% is assumed. In general, bone–cement loosening was easier to detect based on the FRFs as smaller loosened areas could be detected and lower FRAC values were generally found for the same loosened area. The FRAC value for the first loosened area for which the FRAC value is below 0.85 is annotated. FRAC values obtained when 1.5% damping is assumed are presented in a full line box, the FRAC values for the 5% damping cases are presented in a dotted line box. Eg. the minimal loosened area between cement and bone at the anterior side (10(D)) that could be detected based on the FRFs measured on the implant surface was A1 (with a FRAC value of 0.80, obtained at location 4 and a corresponding maximal PSD ratio for that case of 2.1 also obtained at location 4 ) when 1.5% damping was assumed.

**Fig. 11**

The synthesized PSD ratios obtained at all implant measurement locations for the different partial loosening cases are depicted. Ratios above 1.95 are marked light grey, ratios below 1.95 are marked black. Implant locations with high PSD ratios were indicative of nearby loosening. E.g. Locations 7, 8 and 9 show high PSD ratios for the medial loosening case. All three locations are on the side where loosening has occurred. On top of detecting loosening using the FRF feature, the addition of the PSD bandpower feature allows to localize the areas where loosening has occurred.

**Fig.12**

The occurrence of local modal behavior of the implant for partially loosened cases contributes to the increase in PSD bandpower. Fig.12(A) depicts an example of such a local mode for a medial cement–implant loosened case FE model which shows high local deformation. This increase in local deformation is reflected in an increase in PSD bandpower, but is also very visible in the acceleration signal synthesized at measurement location 8. Fig.12(B) shows the synthesized impulse response function (IR, obtained by performing an inverse Fourier transform on the FRF) for a fully cemented FE construct. Fig.12(C) shows the IRF for a L3 partially loosened case. A clear increase in amplitude can be noticed, mainly due to the lower stiffness of the loosened implant–bone construct resulting in the appearance of local modal behavior.

649 **Table 1**

650 The FRAC values and PM – PL PSD ratios are shown for the three different loosening cases. The average
651 FRAC value between the two fully cemented constructs was 0.95; the PM – PL PSD ratio, respectively PL
652 – PM PSD ratio for the fully cemented constructs was 1.06 and 0.95.

653 **Table 2**

654 FRAC values obtained by comparing corresponding 5X FRFs measured on the fully cemented case and on
655 the different loosened cases. Results are shown for all 9 implant measurement locations. The low FRAC
656 values reflect the important differences observed in the vibrational behavior between the fully cemented
657 and loosened cases.

658 **Table 3**

659 The changes in resonance frequencies due to changes in material parameters. The sensitivity is presented
660 as the ratio of a percentage difference in resonance frequencies over a percentage difference of the
661 parameter of interest. E.g. a 10% change in the E33 modulus would result in a 5.4% change in the first
662 resonance frequency.

Figure1

Click here to download high resolution image

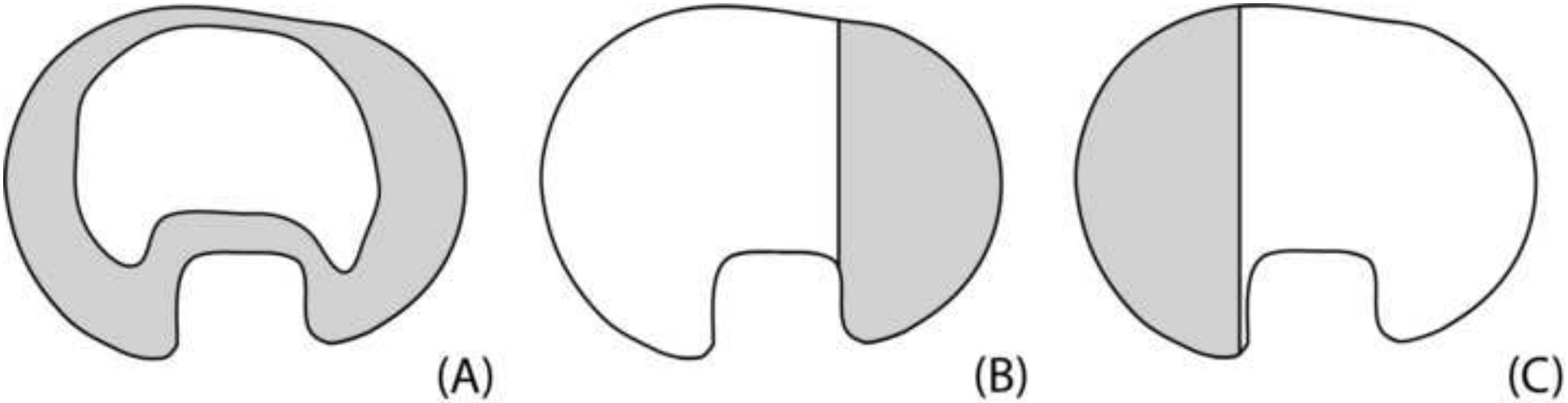

Figure2
Click here to download high resolution image

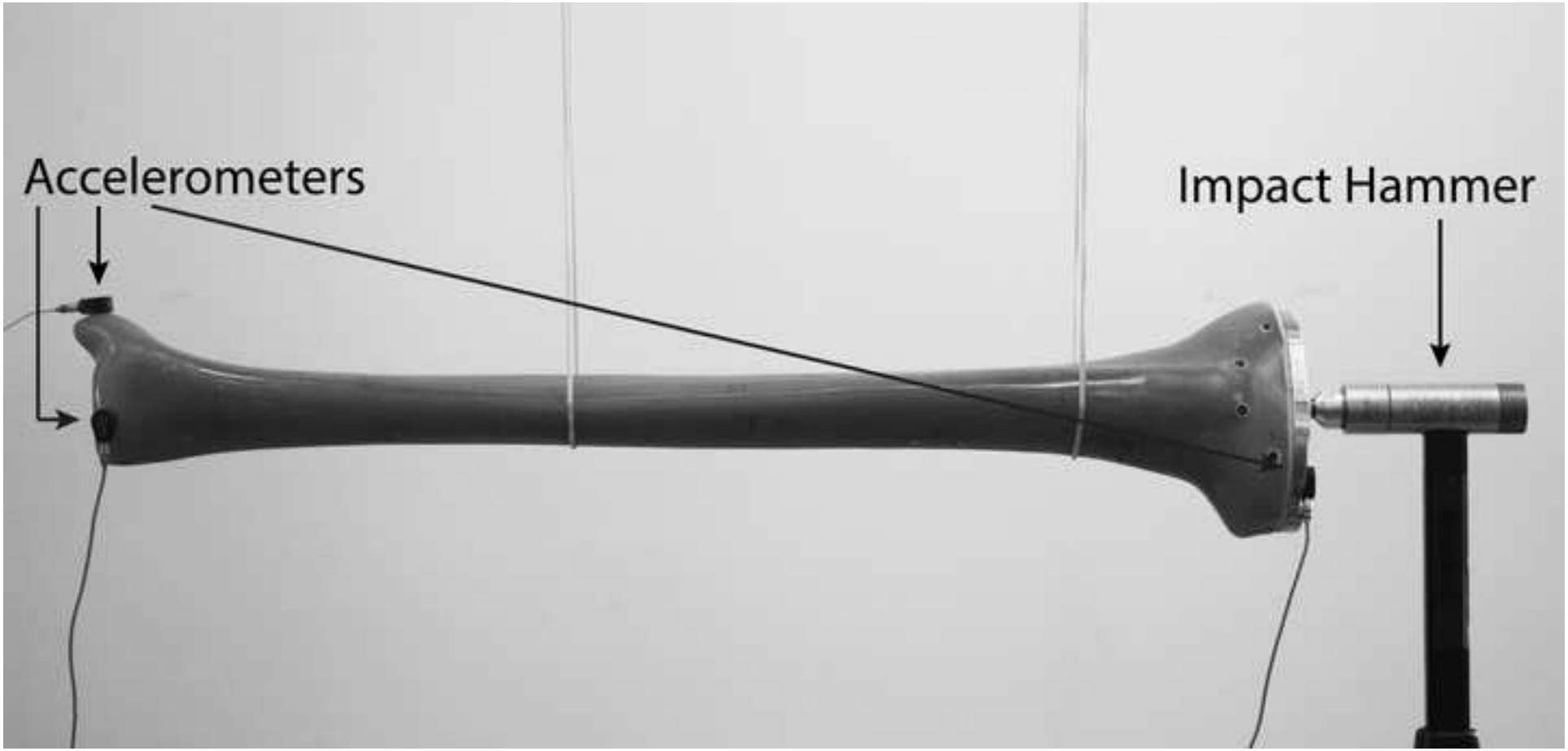

Figure3
Click here to download high resolution image

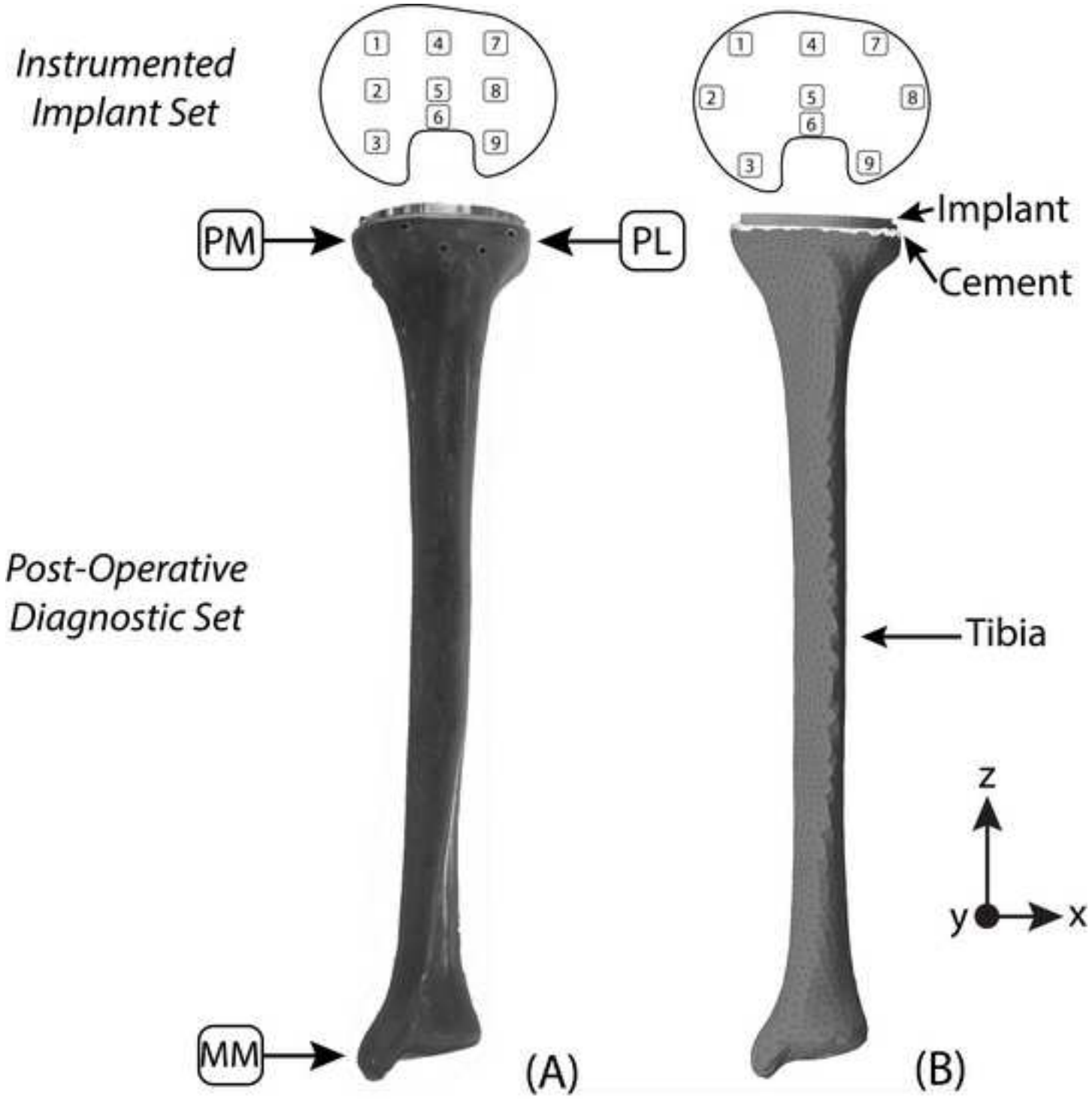

Figure4

Click here to download high resolution image

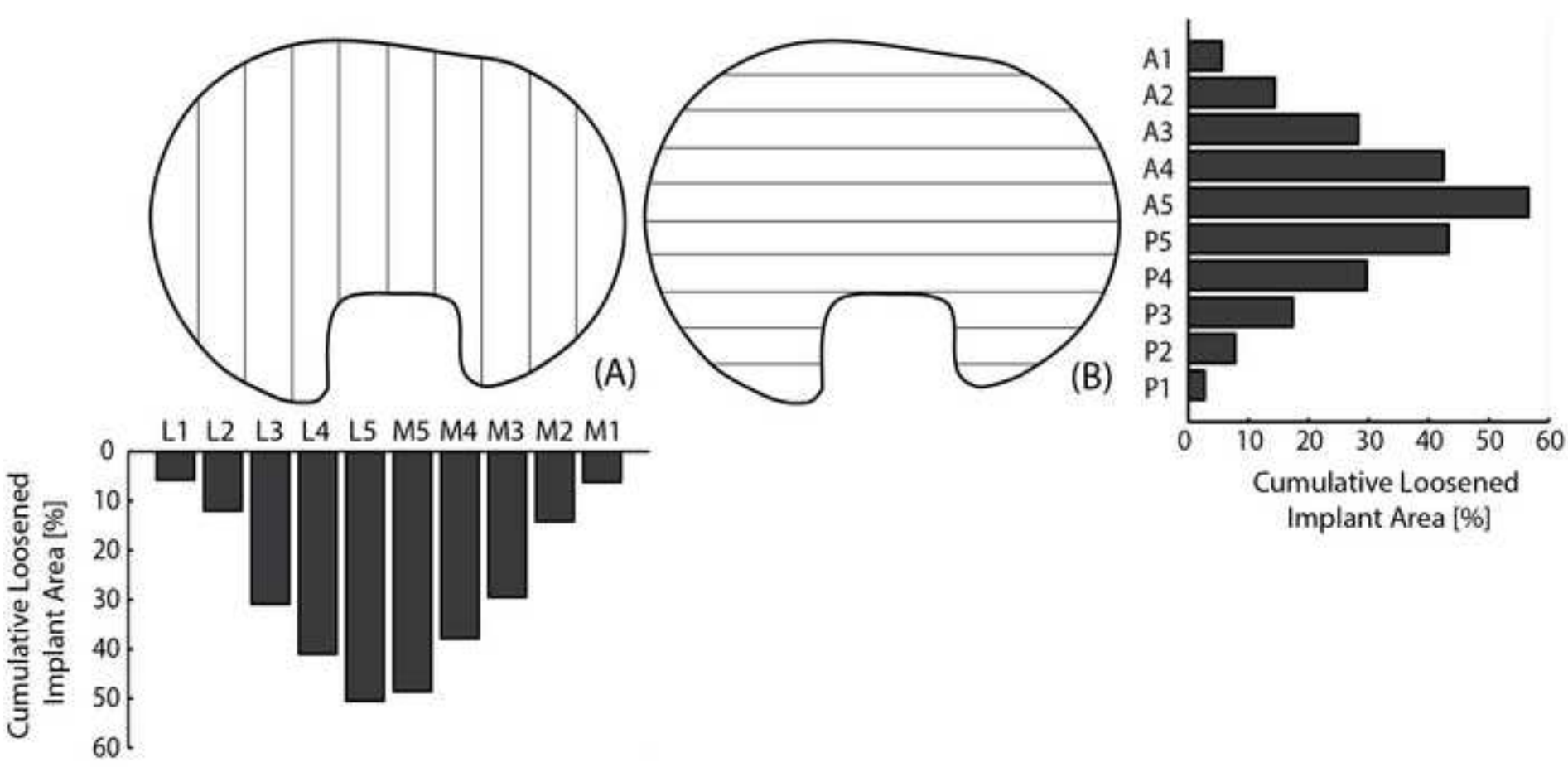

Figure5
Click here to download high resolution image

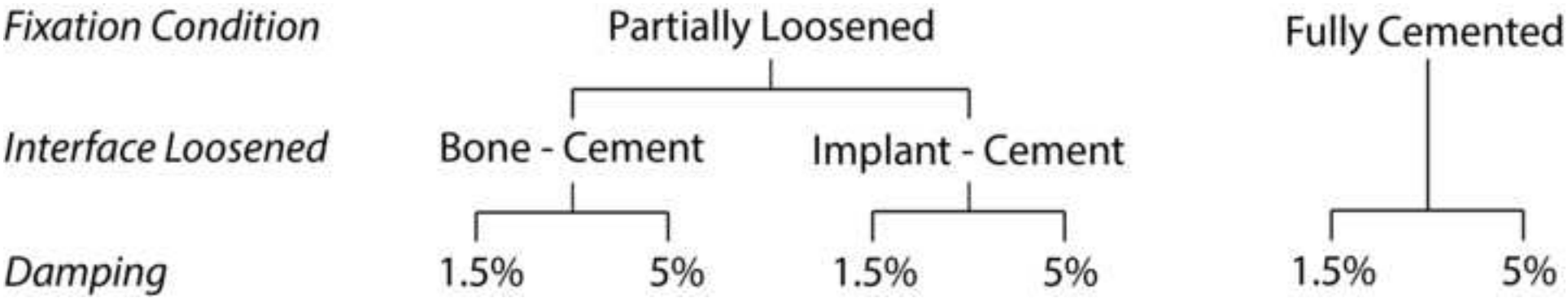

Figure6

Click here to download high resolution image

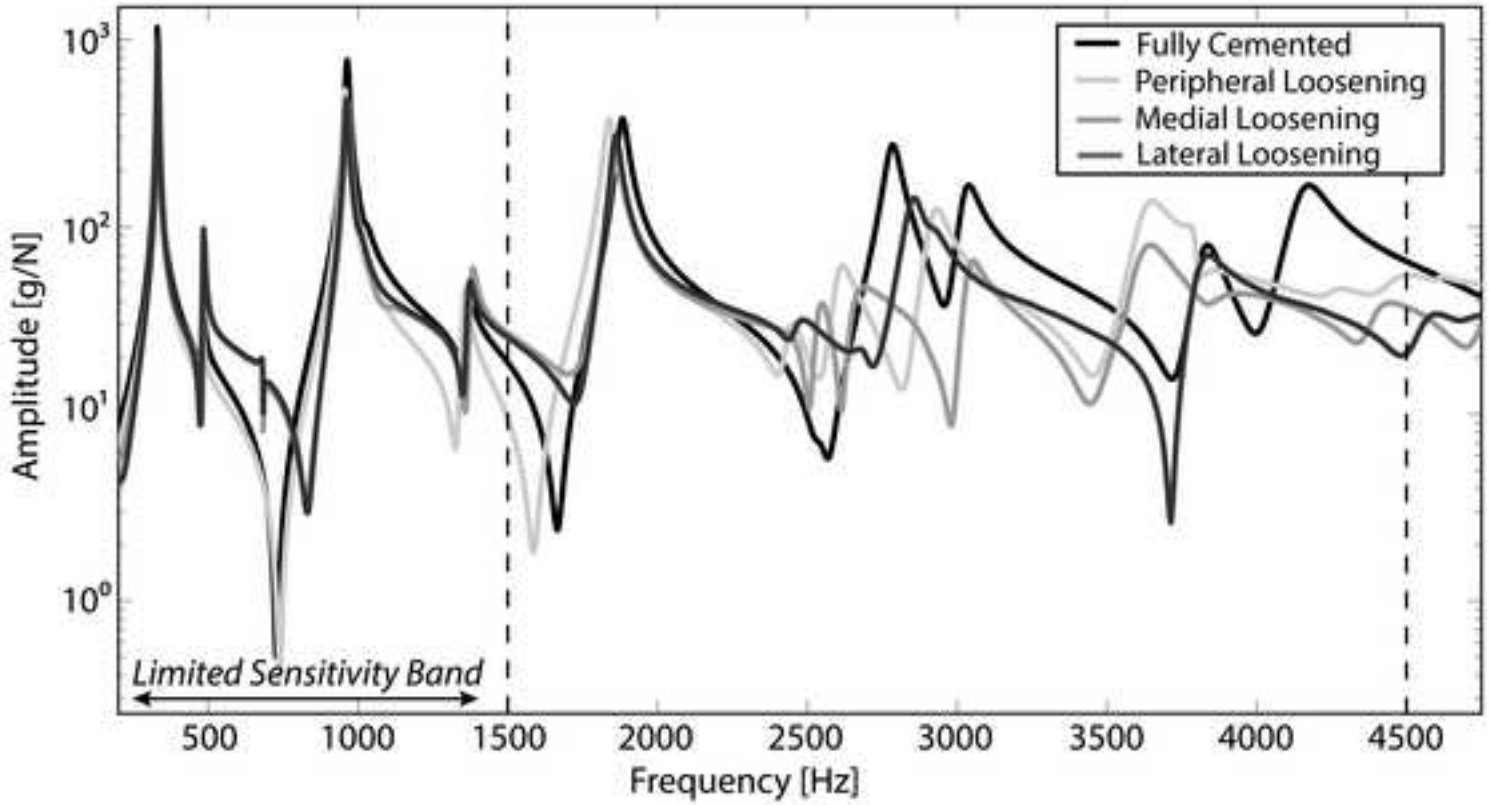

Figure7

Click here to download high resolution image

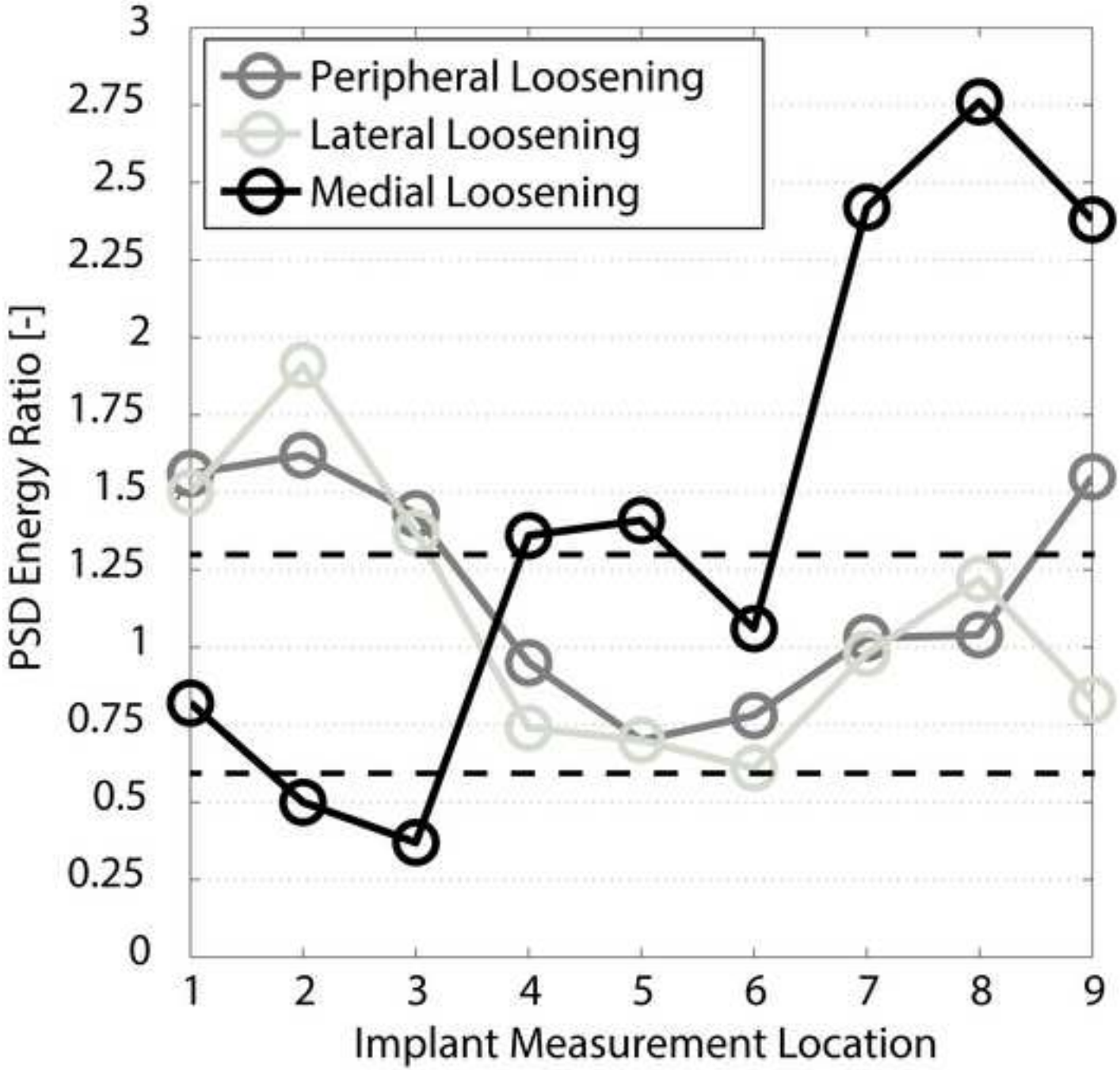

Figure8

Click here to download high resolution image

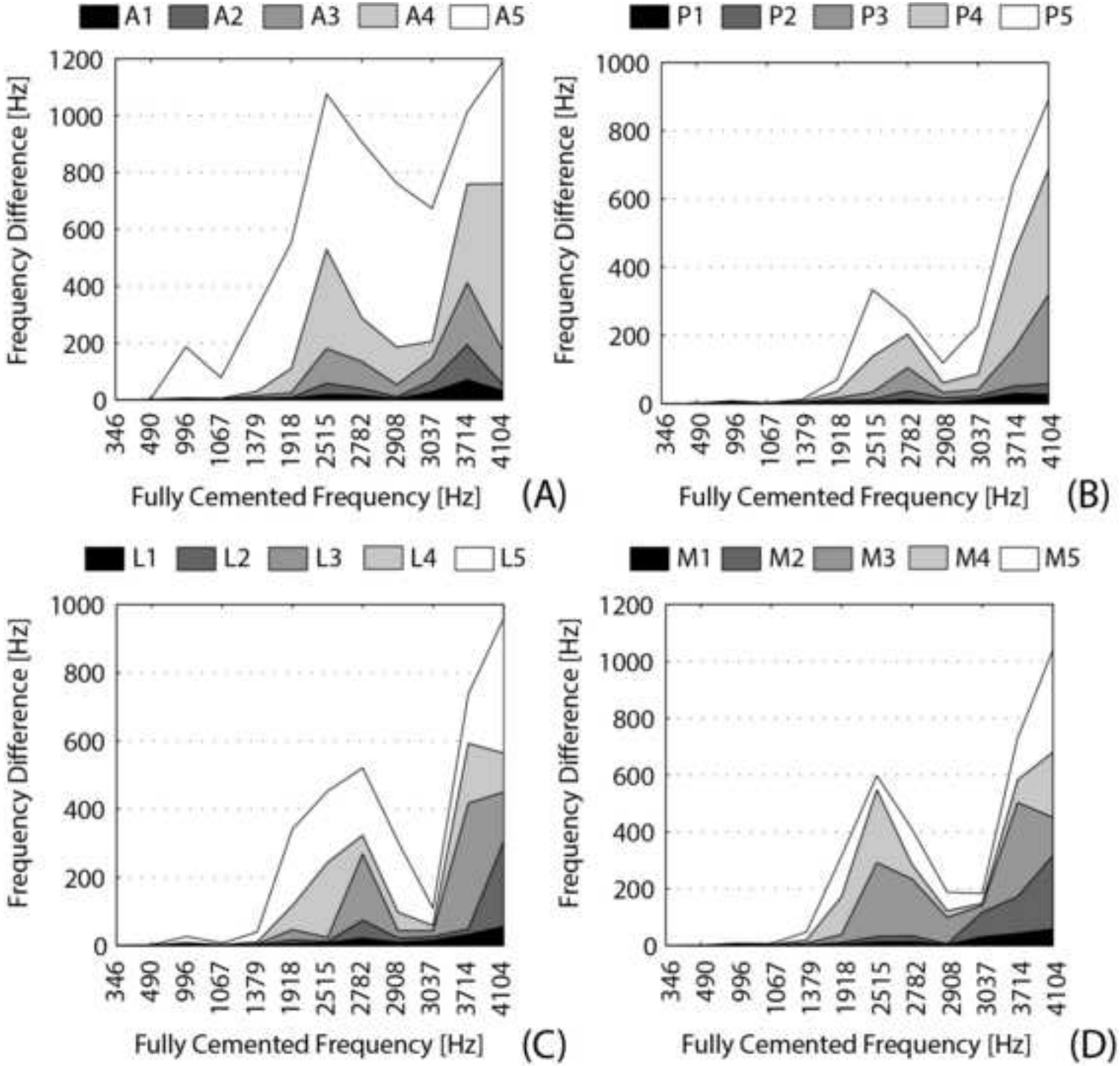

Figure9

Click here to download high resolution image

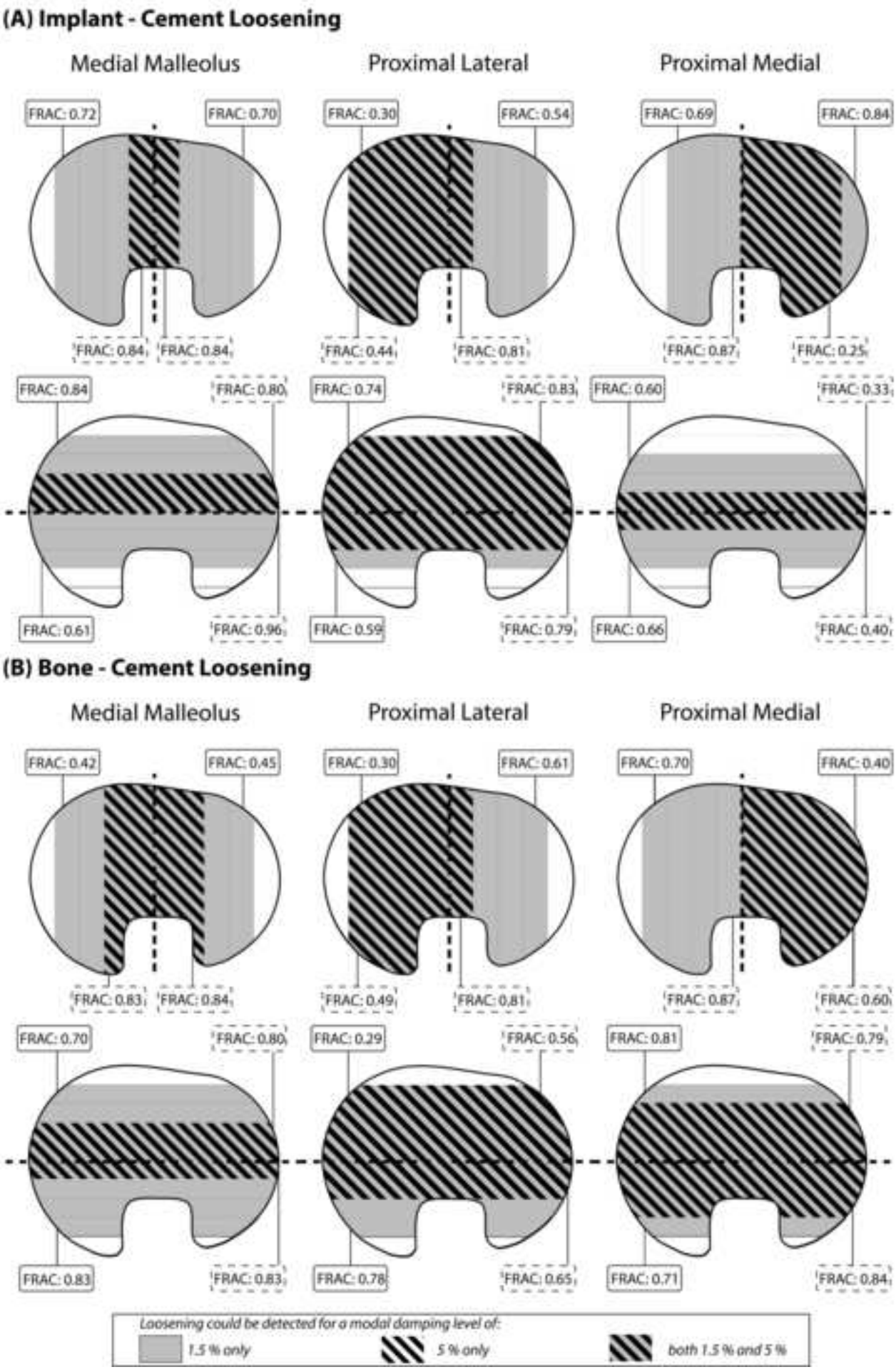

Figure10

Click here to download high resolution image

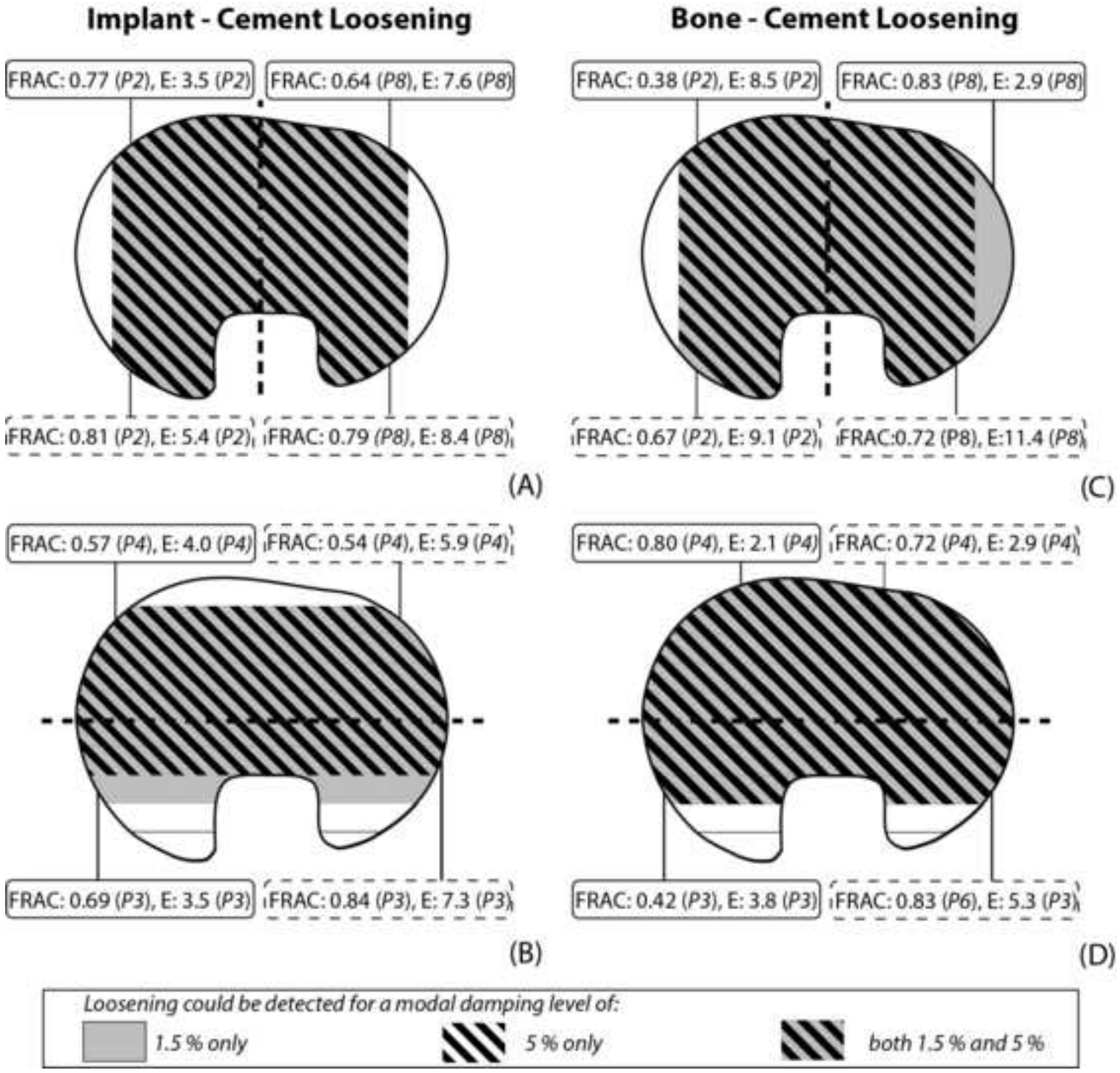

Figure11
Click here to download high resolution image

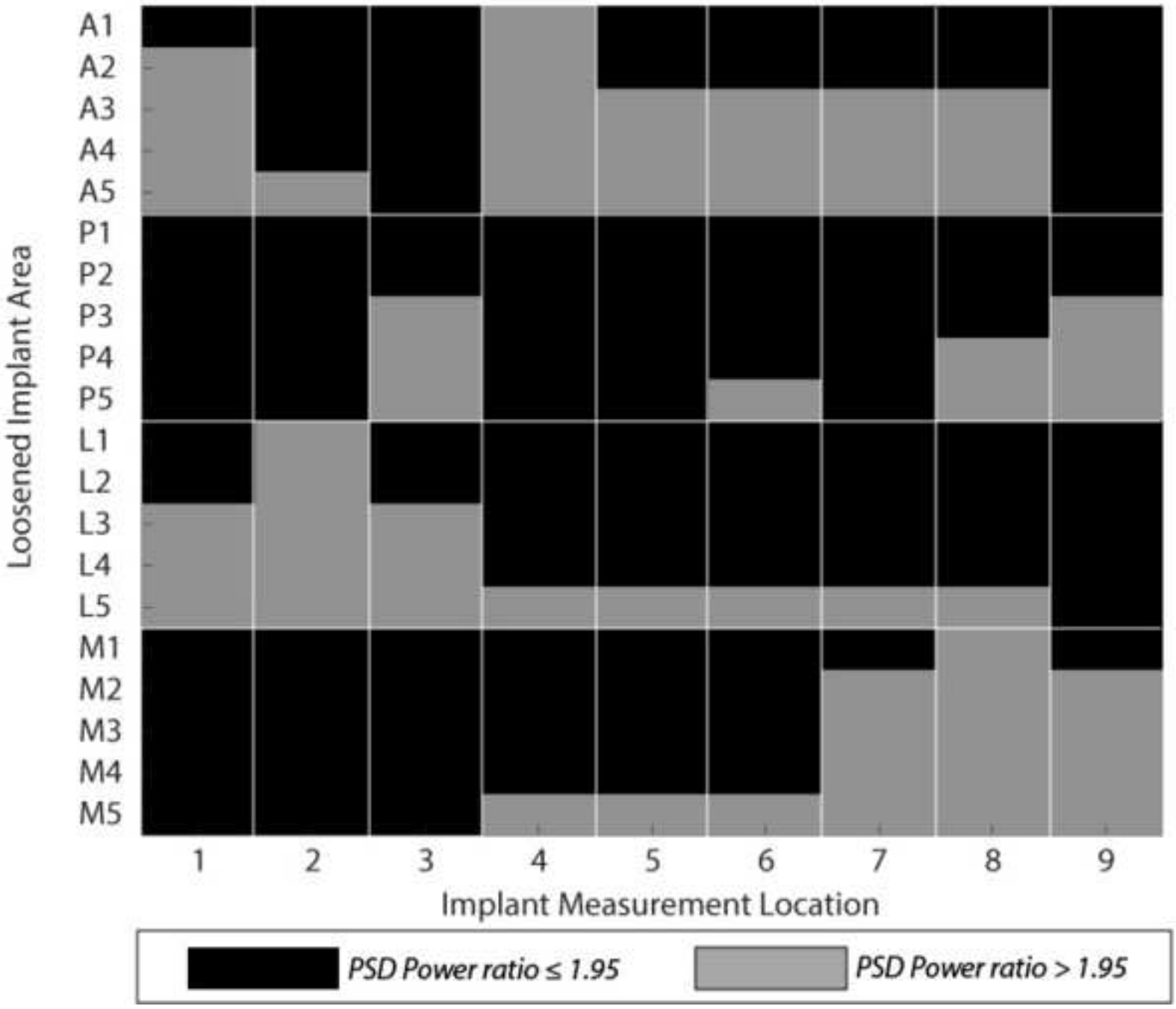

Figure12

Click here to download high resolution image

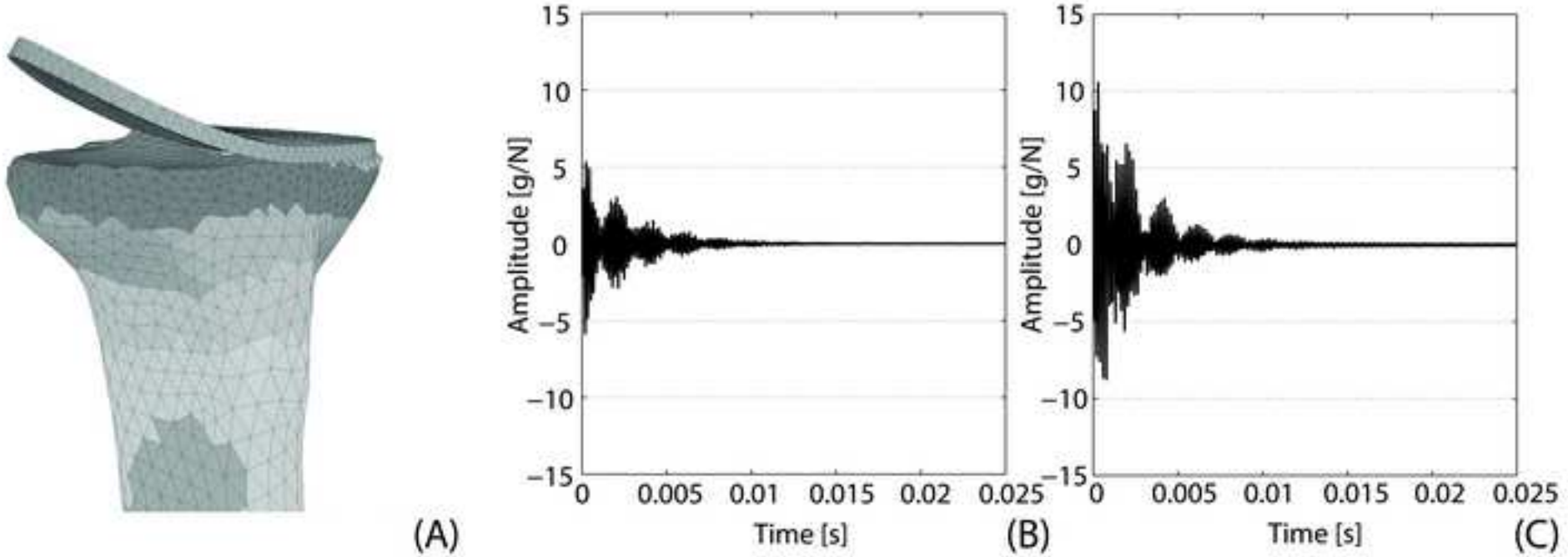

**Table1**

| *Loosening Case* | *FRAC* | | | *Ratio* | |
|---|---|---|---|---|---|
| | PL | PM | MM | PM - PL PSD Ratio | PL - PM PSD Ratio |
| Peripheral Loosening | 0.08 | 0.08 | 0.22 | 0.9 | 1.2 |
| Lateral Loosening | 0.16 | 0.38 | 0.44 | 0.0 | 28.9 |
| Medial Loosening | 0.25 | 0.07 | 0.37 | 101.6 | 0.0 |

**Table2**

| *Measurement Location* | 1 | 2 | 3 | 4 | 5 | 6 | 7 | 8 | 9 |
|---|---|---|---|---|---|---|---|---|---|
| Peripheral Loosening | 0.11 | 0.17 | 0.15 | 0.06 | 0.10 | 0.09 | 0.12 | 0.10 | 0.07 |
| Lateral Loosening | 0.12 | 0.12 | 0.14 | 0.10 | 0.13 | 0.06 | 0.27 | 0.25 | 0.14 |
| Medial Loosening | 0.14 | 0.14 | 0.19 | 0.16 | 0.24 | 0.25 | 0.16 | 0.21 | 0.01 |

**Table3**

| | **Femur % Sensitivities** | | | | | | | | | | | | |
|---|---|---|---|---|---|---|---|---|---|---|---|---|---|
| | Mode Number | 1 | 2 | 3 | 4 | 5 | 6 | 7 | 8 | 9 | 10 | 11 | 12 |
| ***Cancellous*** | E [% GPa] | 0.00 | 0.00 | 0.01 | 0.01 | 0.01 | 0.02 | 0.02 | 0.05 | 0.01 | 0.03 | 0.05 | 0.05 |
| | rho [%] | -0.05 | -0.06 | -0.04 | -0.05 | -0.04 | -0.04 | -0.04 | -0.06 | -0.02 | -0.04 | -0.04 | -0.00 |
| ***Cortical*** | $E_{11} = E_{22}$ [% GPa] | 0.05 | 0.05 | 0.04 | 0.01 | 0.04 | 0.04 | 0.04 | 0.05 | 0.01 | 0.04 | 0.04 | 0.04 |
| | $E_{33}$ [% GPa] | 0.54 | 0.53 | 0.46 | 0.05 | 0.45 | 0.41 | 0.37 | 0.44 | 0.03 | 0.37 | 0.29 | 0.29 |
| | $G_{13} = G_{23}$ [% GPa] | 0.03 | 0.03 | 0.09 | 0.44 | 0.09 | 0.11 | 0.14 | 0.05 | 0.44 | 0.12 | 0.16 | 0.16 |
| | rho [%] | -0.38 | -0.38 | -0.40 | -0.41 | -0.41 | -0.40 | -0.40 | -0.33 | -0.44 | -0.38 | -0.38 | -0.39 |
| ***Cement*** | E [% GPa] | 0.00 | 0.00 | 0.00 | 0.00 | 0.00 | 0.00 | 0.00 | 0.00 | 0.00 | 0.00 | 0.01 | 0.00 |
| | rho [%] | -0.01 | -0.01 | -0.01 | -0.01 | -0.01 | -0.01 | -0.01 | -0.01 | -0.01 | -0.01 | -0.01 | -0.01 |